Available online at www.sciencedirect.com
SCIENCE DIRECT
Biochimica et Biophysica Acta 1713 (2005) 5 – 14
BIOCHIMICA ET BIOPHYSICA ACTA
BBA
http://www.elsevier.com/locate/bba

Structure and thermotropic phase behaviour of detergent-resistant membrane raft fractions isolated from human and ruminant erythrocytes

Peter J. Quinn[a,*], Cedric Tessier[b], Dominique Rainteau[b], Kamen S. Koumanov[c], Claude Wolf[b]

[a]Department of Life Sciences, King's College London, 150 Stamford Street, London SE1 9NN, UK
[b]Faculté de Medecine Saint Antoine, Université Paris 6, INSERM U538, 27 rue Chaligny, Paris 75012, France
[c]Institute of Biophysics, Bulgarian Academy of Sciences, 1113 Sofia, Bulgaria

Received 16 August 2004; received in revised form 26 April 2005; accepted 28 April 2005
Available online 25 May 2005

Abstract

Detergent-resistant membrane raft fractions have been prepared from human, goat, and sheep erythrocyte ghosts using Triton X-100. The structure and thermotropic phase behaviour of the fractions have been examined by freeze-fracture electron microscopy and synchrotron X-ray diffraction methods. The raft fractions are found to consist of vesicles and multilamellar structures indicating considerable rearrangement of the original ghost membrane. Few membrane-associated particles typical of freeze-fracture replicas of intact erythrocyte membranes are observed in the fracture planes. Synchrotron X-ray diffraction studies during heating and cooling scans showed that multilamellar structures formed by stacks of raft membranes from all three species have *d*-spacings of about 6.5 nm. These structures can be distinguished from peaks corresponding to *d*-spacings of about 5.5 nm, which were assigned to scattering from single bilayer vesicles on the basis of the temperature dependence of their *d*-spacings compared with the multilamellar arrangements. The spacings obtained from multilamellar stacks and vesicular suspensions of raft membranes were, on average, more than 0.5 nm greater than corresponding arrangements of erythrocyte ghost membranes from which they were derived. The trypsinization of human erythrocyte ghosts results in a small decrease in lamellar *d*-spacing, but rafts prepared from trypsinized ghosts exhibit an additional lamellar repeat 0.4 nm less than a lamellar repeat coinciding with rafts prepared from untreated ghosts. The trypsinization of sheep erythrocyte ghosts results in the phase separation of two lamellar repeat structures ($d = 6.00$; 5.77 nm), but rafts from trypsinized ghosts produce a diffraction band almost identical to rafts from untreated ghosts. An examination of the structure and thermotropic phase behaviour of the dispersions of total polar lipid extracts of sheep detergent-resistant membrane preparations showed that a reversible phase separation of an inverted hexagonal structure from coexisting lamellar phase takes place upon heating above about 30 °C. Non-lamellar phases are not observed in erythrocytes or detergent-resistant membrane preparations heated up to 55 °C, suggesting that the lamellar arrangement is imposed on these membrane lipids by interaction with non-lipid components of rafts and/or that the topology of lipids in the erythrocyte membrane survives detergent treatment.

Keywords: Erythrocyte raft; Raft structure; Structure of membrane raft; Detergent-resistant membrane

1. Introduction

The creation of lateral and transmembrane domains within biological membranes is known to mediate a wide variety of functions that membranes perform. The interaction between membrane proteins, for example, is believed to underlie the formation of specialized structures such a intercellular junctions and coated pits on the cell surface. While such structures have been examined at the molecular level, the forces governing lipid–lipid interactions in the creation of so-called membrane rafts are less well understood [1–3]. It has been suggested on the basis of model membrane experiments that lateral phase separations take place in membranes enriched in cholesterol, such as the plasma membrane, due to the interaction of cholesterol with saturated molecular species of choline phosphatides to form liquid-ordered phase [4]. The phase is characterized by a

* Corresponding author. Tel.: +44 2078484408; fax: +44 2078484500.
E-mail address: p.quinn@kcl.ac.uk (P.J. Quinn).

0005-2736/$ - see front matter © 2005 Elsevier B.V. All rights reserved.
doi:10.1016/j.bbamem.2005.04.013

relatively close packing of the hydrocarbon substituents, combined with a rapid lateral mobility of the lipid molecules [5]. The driving force for the creation of the phase is believed to be a phase separation of cholesterol from fluid lipids into an association with more saturated molecular species of choline phosphatides, which provide the most energetically favourable shielding of cholesterol from exposure to water [6]. Based on these considerations, the lateral phase separation of liquid-ordered phase is postulated to occur in cell membranes to form lipid rafts [7,8]. Additional interactions between membrane lipids and elements of the cytoskeleton are also thought to be involved [9–11].

The isolation of liquid-ordered domains from biological membranes has been proved possible by exploiting the resistance of such structures to solubilization by detergents such as Triton X-100 [12] and Brij 96 [13]. Fractions that resist solubilization at 4 °C, the so-called detergent-resistant membrane (DRM) fraction, represent membrane rafts. The extent to which membrane rafts reflect the composition and arrangement of constituents in the membrane from which they were derived is conjectural [14,15]. Nevertheless, the composition of DRM fractions from a wide variety of biological membranes has been examined, and they are invariably enriched in sphingomyelin and cholesterol [1,16] and contain proteins characterized by anchorage to the membrane by glycerylphosphoinositide or acyl moieties [17–19]. The composition of DRM fractions differ considerably from the parent membrane [20], and this has led to the suggestion that raft domains are responsible for mediating diverse membrane functions such as signal transduction [18,21–25], protein sorting [2,3,8,26], and membrane budding [27].

There is presently a paucity of information on the structure of DRM fractions from biological membranes to assist in the interpretation of how these functions are performed. The aim of the present study was to isolate DRM fractions from erythrocyte membranes of species with differing sphingomyelin and cholesterol contents and examine their structure and thermotropic phase behaviour. Freeze-fracture electron microscopy shows that DRM fractions are virtually devoid of membrane-associated particles which are characteristic of the intact erythrocyte membranes. Synchrotron X-ray diffraction methods have been used to characterize the structure of erythrocyte ghosts and membrane raft preparations therefrom and to examine the role of membrane proteins in the stability of raft membranes.

2. Materials and methods

2.1. Erythrocyte ghost preparation

Human and ruminant erythrocytes were isolated from fresh citrated blood by procedures described previously [28]. Briefly, whole blood was centrifuged for 10 min at 100×*g*. The erythrocytes were harvested and washed three times with 5 vol. of a buffer consisting of 150 mM NaCl and 5 mM sodium phosphate (pH 8.0) (PBS) and lysed in 40 vol. of 5 mM sodium phosphate (pH 8.0). The resulting membrane ghosts were collected by centrifugation for 20 min at 22,000×*g* and washed four times with lysing buffer to produce 'white ghosts'. When indicated, suspensions of ghost membranes were subjected to digestion with trypsin for 2 h at 37 °C and subsequently washed with PBS.

Detergent-resistant (DRM) fractions were prepared from erythrocyte ghosts by resuspension in a buffer consisting of 0.25 M sucrose, 150 mM NaCl, 1 mM EDTA, and 20 mM Tris–HCl buffer (pH 7.6) containing 1% (v/v) Triton X-100 at 4 °C and by dispersion by 10 passages through a 21-gauge needle. The suspension was diluted with an equal volume of 80% (w/v) sucrose. 4 ml of this detergent-treated membrane suspension was seated in a centrifuge tube and overlaid successively by 4 ml of buffer containing 30% (w/v) sucrose and 3.5 ml of buffer containing 5% (w/v) sucrose. The discontinuous density gradients were centrifuged for 18 h at 38,000×*g* in a SW41 Beckman rotor. The material layered at the 5/30% (w/v) sucrose interface was designated as DRMs and harvested for further examination. Total polar lipid extracts were prepared according to the method of Bligh and Dyer [29] and dispersed in an equal weight of buffer consisting of 0.25 M sucrose, 150 mM NaCl, 1 mM EDTA, and 20 mM Tris–HCl buffer (pH 7.6).

2.2. Freeze-fracture electron microscopy

Suspensions of human erythrocyte ghosts and detergent-resistant membrane fractions were sandwiched between two copper sample mounts (Balzers Union 120557/1205 JT) and equilibrated at 20 °C using a thermally stable gas flow for 3 min prior to thermal quenching. Samples were thermally quenched in a liquid nitrogen jet freezer. Fracturing and replication were performed at −150 °C using a Polaron B7500 freeze-fracture device. Replicas were cleaned in a solvent consisting of chloroform:methanol (2:1, by volume) before examination in a Jeol JEM100CX electron microscope.

2.3. Synchrotron X-ray diffraction

Erythrocyte ghosts were centrifuged at 300,000×*g* for 18 h. Polyvinylpyrrolidone (PVP) powder was added in an equal weight to some pellets to induce stacking of the membranes. DRM were oriented by centrifugation (100,000×*g*, 1 h). Pellets were collected on an aluminium foil seated on the bottom of the centrifuge tubes and transferred to the sample cell sandwiched between a pair of thin mica sheets. The cell was clamped to a thermostated stage (Linkam Scientific Instruments Ltd., UK).

Static powder diffraction patterns were recorded on image plates at beamline BL40B2 at Spring-8, Japan, using

a sample to detector distance of 400 mm and $\lambda = 0.1$ nm. X-ray scattering intensities were obtained by circular integration of the images using FIT2D software, and higher orders of wet rat-tail collagen ($d = 67$ nm) [30] was used to calibrate the spacings. Real-time synchrotron X-ray diffraction experiments were performed using a monochromatic (0.141 nm), focused X-ray beam at beamline 16.1 of Daresbury Synchrotron Radiation Laboratory (Warrington, UK). A website describes in detail the facility available at the station (http://srs.dl.ac.uk/NCD/station161/index.html). X-ray scattering intensities at small angles (SAXS) were recorded using a multiwire quadrant detector at a distance of 2 m from the sample. Wide-angle scattering (WAXS) was recorded using a curved INEL (INstrument ELectronique, France) detector at a distance from the sample of 400 mm. Experimental data were analysed using the OTOKO software [31]. Scattering intensities were corrected for channel detector response using homogeneous irradiation from an ^{55}Fe source. Spatial calibrations were obtained using wet rat-tail collagen. The reciprocal spacing are given as $S = 1/d = 2\sin(\theta)/\lambda$, where d, λ, and θ are repeat distance, X-ray wavelength, and the diffraction angle, respectively.

3. Results

The structure of DRM fractions prepared from erythrocyte ghost membranes was examined by freeze-fracture electron microscopy and synchrotron X-ray diffraction methods. The structure of DRM preparations from human, sheep, and goat erythrocyte ghosts was first compared with intact ghost membranes using freeze-fracture techniques, and the results are shown in Fig. 1. An electron micrograph of an etched human erythrocyte membrane viewed from the outside aspect of the cell (Fig. 1a) shows a characteristic distribution of membrane-associated particles on the P-face, and the etched surface of the cell shows a texture reflecting the arrangement of the underlying particles. Replicas from human DRM (Fig. 1b) show bilayer vesicles and more extensive lamellar structures. The internal bilayer surfaces are smooth and largely devoid of membrane-associated particles; occasionally, small clusters of particles can be seen. Electron micrographs of replicas prepared from suspensions of DRM from sheep (Fig. 1c) and goat (Fig. 1d) are similar to those of suspensions of human detergent-resistant membranes and consist of a mixture of vesicles some of which have more than one layer and extensive stacked sheets of membranes. Again, the texture of the exposed membrane surfaces tends to be smooth and membrane-associated particles are absent. The freeze-fracture data indicate that the original erythrocyte membrane undergoes considerable reorganization as a result of exposure to detergent, and the disruption causes vesiculation and creation of multilamellar arrays of membrane. It is not possible to determine whether or not asymmetric distribution of constituents across the membrane is preserved, but clearly, the constituents responsible for forming membrane-

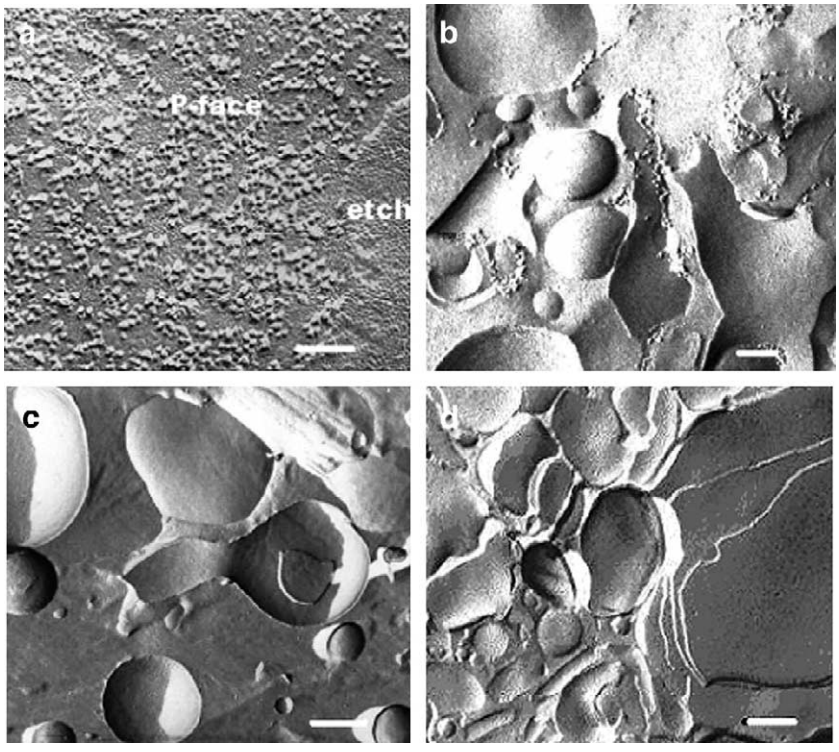

Fig. 1. Electron micrographs of freeze-fracture replicas of (a) etched human erythrocyte membrane and DRM fractions prepared from (b) human, (c) sheep, and (d) goat erythrocyte membranes. Bars = 100 nm.

associated particles are either rearranged or excluded from the membrane.

The structure and thermotropic phase behaviour of DRM fractions from human and ruminant erythrocytes was examined by real-time synchrotron X-ray diffraction methods. Heating and cooling scans were performed to aid in the assignment of the diffraction peaks. A sequence of X-ray scattering intensity profiles recorded from a preparation of human DRM heated from 10 °C to 50 °C is shown in Fig. 2A. This shows the SAXS region of the scattering intensity profile in which a relatively sharp reflection at about 6.7 nm and a broader band at about 5.4 nm can be seen at 10 °C. The peak at 6.7 nm shifts progressively to lower *d*-spacings in concert with a minor peak at about 3.3 nm (Fig. 2A; arrow) upon heating from 10 °C to 50 °C (Fig. 2B). Both peaks undergo a corresponding increase in *d*-spacing during subsequent cooling, indicating that the structural changes are reversible (data not shown). These two spacings are assigned to the first- and second-order reflections from a multilamellar structure. The maximum intensity of the first-order reflection (Fig. 2C) increases during the scan as the peak becomes sharper. The relatively broad peak at about 5.4 nm, by contrast, expands during the heating scan (Fig. 2B) and contracts during cooling (data not shown), indicating that this reflection originates from a different structure. No higher-order reflections of this peak could be detected, but the most likely origin of this reflection is that it originates from unstacked bilayers, presumably vesicles. The WAXS profiles show broad reflections at a spacing of 0.45 nm throughout the temperature scans, consistent with a disordered hydrocarbon phase (data not shown).

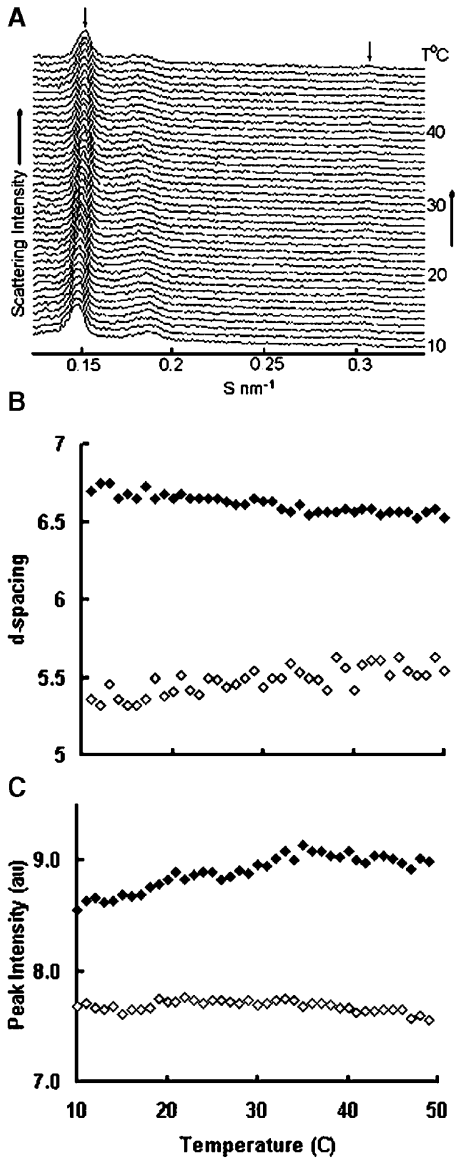

Fig. 2. (A) Small-angle X-ray scattering intensity patterns recorded from a suspension of human erythrocyte detergent-resistant membranes during a heating scan between 10 °C and 50 °C at 1°/min. The temperature interval of each of diffraction pattern is 1 °C. Arrows indicate the first and second orders, respectively, of a lamellar repeat structure. The temperature dependence of *d*-spacings (B) and the relative X-ray scattering intensities (C) of the first-order lamellar repeat (♦) and broad scattering band (◇) recorded during the heating scan are shown.

The results obtained from a heating scan of a preparation of DRM from sheep erythrocytes is shown in Fig. 3. The X-ray scattering profile at the initial temperature shows a single relatively broad scattering band centred at a spacing of about 5.6 nm (Fig. 3A). The position of this band decreases by about 0.1 nm during heating to 55 °C (Fig. 3B). A new peak at about 6.8 nm appears during the scan at about 30 °C, and the spacing decreases progressively to about 6.2 nm at 55 °C. There is a decrease in scattering intensity of the peak centred at 5.6 nm and a corresponding increase in the intensity of the new peak during the heating scan (Fig. 3C). The two X-ray scattering bands cannot be assigned to lamellar structures, as no higher-order reflections can be detected, and because they show different dependence on temperature, the scattering is likely to originate from different structures. Based on the position of the peaks, a provisional assignment is a vesicular arrangement of DRM indexed by the spacing at 5.6 nm, which stacks into multilamellar structures at temperatures greater than 30 °C. The WAXS profiles were dominated by a broad temperature-independent diffraction band centred at 0.45 nm in both heating and cooling scans.

A sequence of SAXS intensity profiles from a preparation of goat DRM recorded during a heating scan from 15 °C to 45 °C is shown in Fig. 4A. A sharp peak at about 6.7 nm at 15 °C is assigned to the first-order reflection of a multilamellar phase indexed by two orders of reflection. These spacings decrease progressively to 6.10 nm at 45 °C. A relatively broad band at a spacing corresponding to about 4.9 nm appears at about 25 °C (Fig. 4B) and increases in intensity during the remainder of the heating scan (Fig. 4C). No higher-order reflections can be detected from this scattering band, but a decrease in scattering intensity from the multilamellar array is consistent with the formation of vesicles of DRM upon heating above 25 °C. The process of vesiculation was found to be completely reversible during a

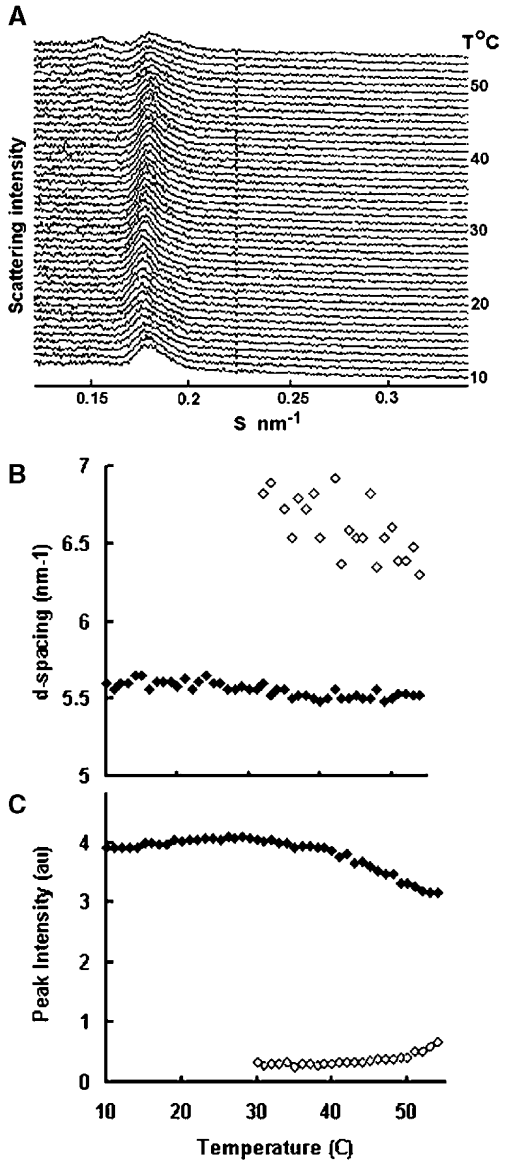

Fig. 3. (A) Small-angle X-ray scattering intensity patterns recorded from a suspension of sheep erythrocyte detergent-resistant membranes during a heating scan between 10 °C and 55 °C at 1°/min. The diffraction patterns are plotted at intervals of 1 °C. The temperature dependence of *d*-spacings (B) and the relative X-ray scattering intensities (C) from the major diffraction peak (♦) and the emergent diffraction band (◊) recorded during the heating scan are shown.

subsequent cooling scan (data not shown). Like the DRM from human and sheep, the WAXS profile showed a temperature-independent scattering band centred at about 0.45 nm.

The effect of membrane protein on the structure and stability of erythrocyte ghosts and detergent-resistant membranes was investigated. The experimental approach was to subject the ghost membranes to digestion with trypsin and to examine the static X-ray structure of the trypsinized membranes and detergent-resistant membrane fractions isolated from the membranes. The results for human erythrocytes are presented in Fig. 5. This shows that a suspension of control and trypsinized erythrocytes formed into multilamellar structures by the addition of PVP give almost identical repeat spacings of about 5.9 nm (Fig. 5A). Detergent-resistant membrane preparations formed into multilamellar stacks by centrifugation from control and trypsinized erythrocytes show different diffraction profiles (Fig. 5B). The control raft shows a single lamellar repeat corresponding to 6.55 nm (the peak at 5.5 nm is the scattering band from vesicles), whereas the membranes derived from trypsinized ghosts form two lamellar structures

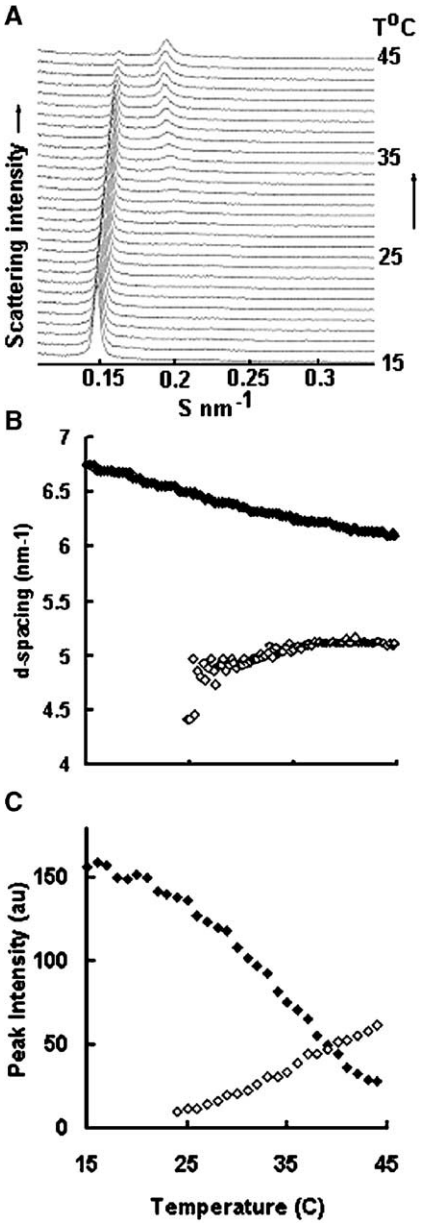

Fig. 4. (A) Small-angle X-ray scattering intensity patterns recorded from a suspension of goat erythrocyte detergent-resistant membranes during a heating scan between 15 °C and 45 °C at 1°/min. The diffraction patterns are plotted at intervals of 1 °C. The temperature dependence of *d*-spacings (B) and the relative X-ray scattering intensities (C) from the major diffraction band (♦) and the emergent diffraction band (◊) recorded during the heating scan are shown.

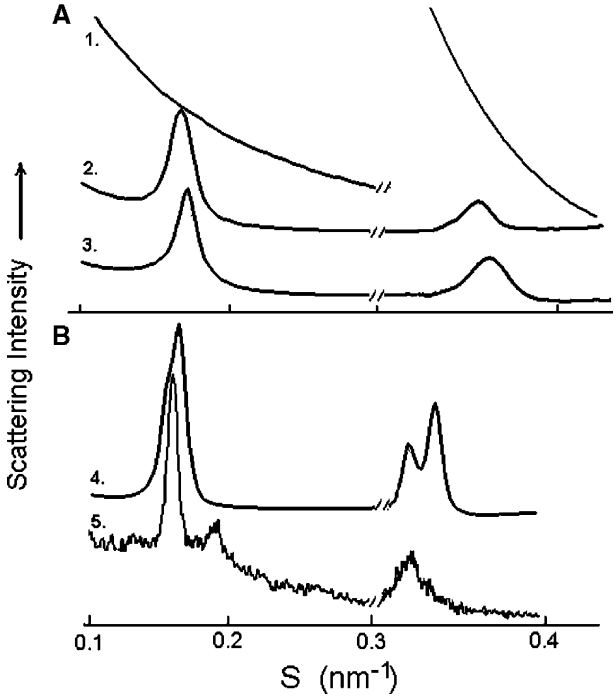

Fig. 5. Effect of tryptic digestion on the structure of human erythrocyte ghost membranes and detergent-resistant membranes derived therefrom. Static small-angle X-ray scattering intensity profiles recorded at 37 °C from human erythrocyte ghosts (A) concentrated by ultracentrifugation (curve 1) and after the addition of PVP to ghost membranes untreated (curve 2) or digested by trypsin (curve 3) are shown. (B) Detergent-resistant membranes prepared from trypsin-digested ghosts (curve 4) and untreated ghosts (curve 5). The scattering intensity above $S=0.3$ nm^{-1} has been scaled to emphasize the weaker scattering peaks.

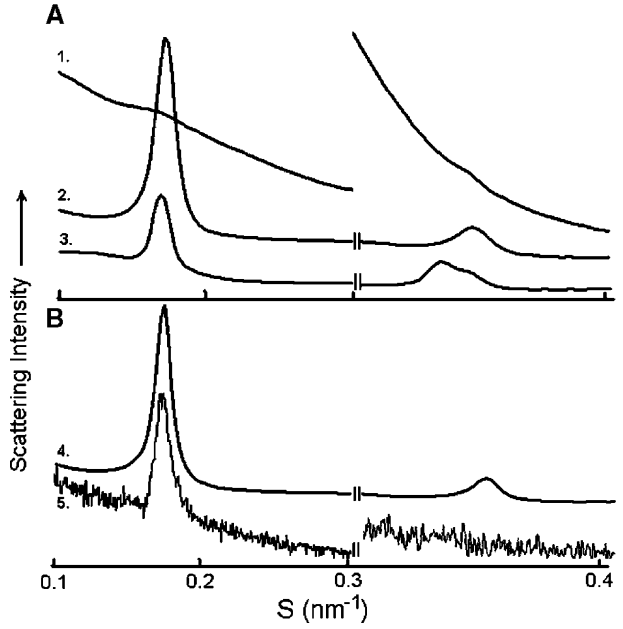

Fig. 6. Effect of tryptic digestion on the structure of sheep erythrocyte ghost membranes and detergent-resistant membranes derived therefrom. Static small-angle X-ray scattering intensity profiles recorded at 37 °C from sheep erythrocyte ghosts (A) concentrated by ultracentrifugation (curve 1) and after the addition of PVP to a suspension of ghost membranes untreated (curve 2) or digested by trypsin (curve 3) are shown. (B) Detergent-resistant membranes prepared from trypsin-digested ghosts (curve 4) and untreated ghosts (curve 5). The wide-angle scattering intensity has been scaled to emphasize the weaker scattering peaks.

of *d*-spacings 6.51 and 6.15 nm, respectively. This result suggests that the removal of protein from the ghost membrane by trypsin causes the formation of detergent-resistant membrane structures with a smaller *d*-spacing than those from untrypsinized ghosts.

The effect of trypsin treatment of sheep erythrocyte ghosts is different from that of human membranes (Fig. 6). With sheep ghosts, trypsinization results in phase separation of the ghost membrane evidenced by the presence of two lamellar repeats in membranes stacked by the presence of PVP (Fig. 6A). By contrast, the lamellar repeat spacings of detergent-resistant membranes from control and trypsinized ghosts is almost identical. This result suggests that trypsinization alters the structure of the erythrocyte ghost membrane, but because most of the membrane of this species is in a liquid-ordered phase, fractionation by detergent is unaffected by the removal of protein from the parent membrane.

From these results and those from the temperature scans, a comparison of the *d*-spacings recorded from the different membranes at 37 °C has been collated in Table 1. It can be seen that the spacings obtained from multilamellar stacks and vesicular suspensions of raft membranes were, on average, more than 0.1 nm greater than corresponding arrangements of erythrocyte ghost membranes from which they were derived.

The effect of membrane protein on the structure of the lipid was investigated by comparing the thermal stability of sheep DRM (Fig. 3) with the thermotropic phase behaviour of the dispersions of total lipid extracts prepared from sheep DRM. The SAXS and WAXS intensity patterns recorded from a lipid dispersion during a heating and subsequent cooling scan identical to that of DRM preparation shown in Fig. 3 are presented in Figs. 7A and B, respectively. The dispersion forms multilamellar structures at all temperatures covered by the thermal scan with a *d*-spacing indexed by two orders of reflection of 5.7 nm at 50 °C. Upon heating above 30 °C, a non-lamellar phase emerges from the multilamellar structure; this phase has a *d*-spacing at 50 °C of 6.1 nm indexed by three orders of reflection in a space grouping: 1, $1/\sqrt{3}$, and $1/\sqrt{4}$ (see arrows). The higher orders of reflection of the non-lamellar phase are illustrated in the static patterns recorded at 34 °C and 50 °C plotted on a

Table 1
Spacings (nm) of erythrocyte membrane preparations from different species obtained from X-ray scattering intensity bands recorded at 37 °C

Species	Multilamellar		Vesicles	
	Ghosts[a]	DRM	Ghosts	DRM
Human	6.00	6.10	4.93	5.15
Sheep	5.78	6.02	5.10	5.08
Goat	n/d	6.02	n/d	5.01

[a] In the presence of PVP.

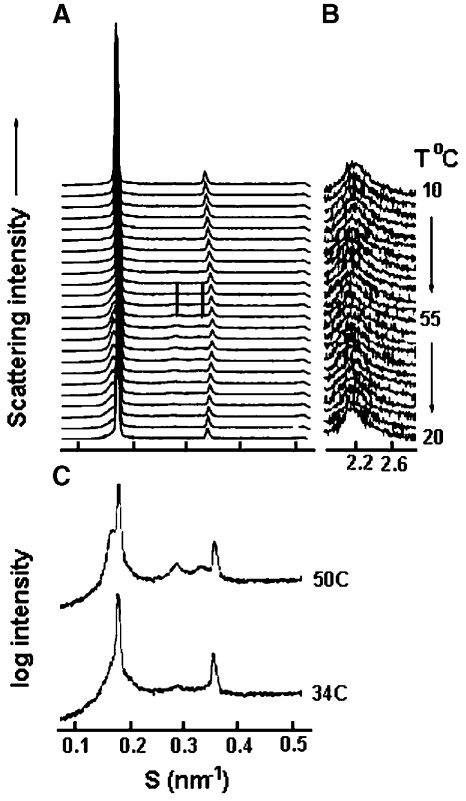

Fig. 7. Small-angle (SAXS) (A) and wide-angle (WAXS) (B) intensity patterns recorded from an aqueous dispersion of a total polar lipid extract of sheep DRM during a heating scan from 10 °C to 55 °C and a subsequent cooling scan to 20 °C at 1°/min. (C) SAXS intensity patterns recorded at designated temperatures recorded during an initial heating scan plotted on a logarithmic scale.

logarithmic scale in Fig. 7C. The result is interpreted as the coexistence of lamellar and hexagonal-II phases at temperatures greater than 30 °C; the phase separation is reversed on subsequent cooling to 10 °C. The *d*-spacing has a value of 5.80 nm at 37 °C and compares with a value of about 6.02 nm for multilamellar arrangements of sheep erythrocyte DRM suspensions (Table 1).

4. Discussion

The DRM preparations from erythrocyte ghost membranes are predominantly in the form of vesicles of variable size, as seen from the freeze-fracture electron microscopic evidence. In addition to vesicles, the presence of multilamellar arrangements indicates that considerable rearrangement takes place as a result of exposure of the ghost membrane to Triton X-100 at 4 °C. From an operational viewpoint, it is important determine to what extent the DRM preparations accurately reflect the topological arrangement of the components of the parent membrane. One obvious and common feature of all the DRM preparations is the virtual absence of membrane-associated particles from the inner fracture plane. This is consistent with the presence of a liquid-ordered structure of the hydrocarbon chains from which components that comprise these membrane-associated particles are often excluded. The exclusion of transmembrane peptides from DRM is believed to be due to the tight packing of the hydrocarbon chains associated with the formation of liquid-ordered phase [32,33]. A similar exclusion of membrane-associated particles is observed in biological membranes cooled to temperatures below the gel phase transition of the constituent lipids [34]. It is often inferred that the phase separation involves a lateral phase separation of intrinsic membrane proteins from the ordered lipid bilayer, but an analysis of the membrane-associated particle density leads to the conclusion that intrinsic proteins may be ejected from the hydrophobic region of the bilayer (vertical displacement) or that the constituents of the particles become rearranged in such a way as to be accommodated within the hydrophobic domain of the ordered lipid bilayer [35].

The X-ray scattering intensity patterns obtained from unoriented vesicles of biological membranes are interpreted as reflections arising predominantly from the lipid bilayer matrix [36]. The repeat structure consists of two layers of relatively high electron density representing the lipid–water interface, where the polar phosphate groups of the membrane lipids reside and which sandwich a layer of relatively low electron density where the hydrocarbon chains are located [37,38]. X-ray scattering intensity profiles from a variety of biological membranes, including rat erythrocytes, were found to consist of broad diffraction bands centred at about 5 nm, with occasionally higher-order reflections. The broad scattering from these preparations was believed to be due to interference within the bilayer rather than a broadened Bragg reflection resulting from inter-membrane interference. The first-order scattering peak from such membranes is anomalous and does not correspond to the bilayer thickness; however, higher-order scattering maxima are used as a reliable measure of the distance separating the phosphate groups on either side of the bilayer [39,40]. No higher-order peaks from vesicular suspensions could be detected from the synchrotron X-ray study, but the assignment of the single broad scattering intensity maxima at spacings about 5 nm to the continuous transform of single unstacked bilayers could be made from the relative position of the peak and the difference in temperature dependence of these peaks with respect to those that could be unambiguously assigned to stacked multilayers. The temperature dependence of DRM forming these two structures differed with the species of red cell. Thus, goat DRM tended to form multilamellar arrangements at temperatures below about 25 °C, and these destacked to form vesicles at higher temperatures. Sheep DRM showed the opposite behaviour in that vesicles were the only structure observed at temperatures below 30 °C, and these tended to stack into a smectic phase at higher temperatures. Human DRM preparations formed a mixture of stacked arrays and vesicles, the proportion of which remained relatively constant over the temperature

range 10 °C to 50 °C. The reasons for these differences in macroscopic behaviour are presently unknown.

An examination of the corresponding WAXS profiles of DRM preparations from all species indicated a broad scattering band at all temperatures investigated consistent with disordered hydrocarbon chains. The detection of ordered lipid phases on the basis of wide-angle X-ray scattering data is problematic [41], but the existence of liquid-ordered lipid phase is likely on the basis of the high content of saturated molecular species of sphingomyelin and cholesterol present in DRM preparations from erythrocyte membranes [20].

The influence of the extrinsic component of membrane proteins on the structure of human erythrocytes differs from sheep. The digestion of human erythrocytes with trypsin is known to release about 90 proteins with unique sequences from the cytoplasmic and exoplasmic surfaces of the membrane [42]. The only detectable effect of the treatment of the erythrocyte ghost was a reduction of about 3% in the lamellar repeat spacing of membranes stacked in the presence of PVP. The removal of protein, however, resulted in a significant change in the structure of DRM prepared from digested membranes. Two components distinguished by their lamellar *d*-spacing were observed, one with a *d*-spacing almost identical to DRM prepared from undigested erythrocyte membranes and the other with a significantly lower *d*-spacing. Since Triton X-100 is believed to fractionate membranes on the basis of solubility of the membrane lipids, this result would suggest that the proteins that accompany the insoluble lipids influence the structure of the DRM. The creation of two distinct DRM fractions indicates that either DRM derived from trypsinized membranes contain a different set of proteins or that the polypeptides that survive tryptic digestion that turn up as components of the DRM have been segregated within the membranes. By contrast, trypsinization of sheep erythrocyte ghosts causes perturbation of the structure, as evidenced by the creation of membranes exhibiting a new *d*-spacing somewhat greater than that observed in untreated membrane. The reason for this species difference may be due to the recovery of only 5% of the total membrane lipid in the human DRM fraction, whereas in sheep, this fraction represents 35% of the total ghost lipid [20]. Any specific effects of protein on the *d*-spacing of raft domains in human ghost membranes would be difficult to detect compared with sheep ghosts, in which liquid-ordered lipid phase represents a significant component of the total erythrocyte membrane. There is no evidence of segregation of protein domains in the DRM fraction prepared from trypsinized sheep ghost membranes, as a single *d*-spacing is observed which coincides with DRM fractions prepared from native erythrocyte ghosts.

A comparison of the thermotropic behaviour of DRM preparations from sheep erythrocytes with that of aqueous dispersions of total polar lipids extracted from the DRM provides insight into the role of the non-lipid components on the structure and stability of the rafts. The emergence of a non-bilayer phase is induced in lipid dispersions when the temperature exceeds about 30 °C. The phase behaviour is completely reversible, indicating that interaction with other bilayer-forming lipids or non-lipid constituents does not interfere with the phase separation involved in the transition. The membrane lipids most likely to form hexagonal-II structure are the unsaturated molecular species of phosphatidylethanolamines, which are known to phase separate from cholesterol in bilayer phases [43]. By contrast, no non-bilayer lipid structures can be detected in DRM preparations, even at temperatures of 50 °C. This can be explained if the non-lipid components that are removed during extraction interact with non-bilayer forming lipids to impose a bilayer configuration. Alternatively the topography of the lipids in the DRM fractions is not preserved in the dispersed lipid extract in which a random distribution of lipids would be expected. The possibility that both factors are responsible for the stability of the DRM also cannot be excluded.

One theory to explain a putative function of membrane rafts can be assessed from the results presented in Table 1. The creation of lipid rafts in the midst of the generally disordered membrane lipid matrix [2,22,44] is believed to act as a selective protein filter admitting only those proteins whose membrane insertion is specifically adapted to ordered lipids [45,46]. A mechanism that has been proposed to achieve this adaptation is that the hydrophobic span of intrinsic proteins is longer and said to be matched to the thicker hydrocarbon length of liquid-ordered phases [8,47]. Support for this theory was reported from the results of X-ray diffraction studies of model systems in which the hydrocarbon thickness of lipid mixtures that resist solubilization by Triton X-100 was determined from electron density calculations [48]. While it is known that bilayer thickness may not be related to *d*-spacings and that differences in water layer thickness may be influenced by differences in the composition of the membranes, the present results show consistently greater *d*-spacings for DRM arrays compared with erythrocyte ghosts from which they were prepared. The same trend was also seen in the position of the scattering band observed in vesicular dispersions. Recent evidence also points to membrane proteins as determinants of bilayer thickness and not cholesterol, as is often assumed [40]. Again, a comparison of the *d*-spacing of sheep DRM with dispersions of lipid extracts of the DRM is consistent with this evidence, although it must be emphasized that proteins may influence water layer thickness. Clearly, also the presence of protein on the membrane surface may be a factor because differences in thickness of about 0.4 nm between the Lo and Lα phases have been reported in mixed lipid systems on the basis of atomic force microscopic measurements [49]. While differences in bilayer thickness may distinguish fluid from liquid-ordered phases, this may not be the only factor related to the mechanism responsible for protein sorting. In model studies of peptides with lengths tailored to span the width of

fluid or liquid-ordered bilayers, it was found that neither type of peptide colocalizes in DRM fractions, suggesting that the cohesive properties of the bilayer may be of greater significance than hydrophobic match in the sorting of transmembrane peptides [32,33].

Acknowledgements

The synchrotron X-ray diffraction experiments were assisted at the Daresbury SRS by Dr. Anthony Gleeson and by Drs. H. Takahashi, K. Inoue and S. Ueno at Spring-8 (2004B0248-NL2a-np). Freeze-fracture electron microscopic studies were ably assisted by Dr. Tony Brain.

References

[1] D.A. Brown, E. London, Structure and function of sphingolipid- and cholesterol-rich membrane rafts, J. Biol. Chem. 275 (2000) 17221–17224.
[2] K. Simons, E. Ikonen, Functional rafts in cell membranes, Nature 387 (1997) 569–572.
[3] K. Simons, E. Ikonen, How cells handle cholesterol, Science 290 (2000) 1721–1726.
[4] J.H. Ipsen, G. Karlstrom, O.G. Mouritsen, H. Wennerstrom, M.J. Zuckermann, Phase equilibria in the phosphatidylcholine-cholesterol system, Biochim. Biophys. Acta 905 (1987) 162–172.
[5] O.G. Mouritsen, Theoretical models of phospholipid phase transitions, Chem. Phys. Lipids 57 (1991) 179–194.
[6] J. Huang, G.W. Feigenson, A microscopic interaction model of maximum solubility of cholesterol in lipid bilayers, Biophys. J. 76 (1999) 2142–2157.
[7] S.N. Ahmed, D.A. Brown, E. London, On the origin of sphingolipid/cholesterol-rich detergent-insoluble cell membranes: physiological concentrations of cholesterol and sphingolipid induce formation of a detergent-insoluble, liquid-ordered lipid phase in model membranes, Biochemistry 36 (1997) 10944–10953.
[8] M.S. Bretscher, S. Munro, Cholesterol and the Golgi apparatus, Science 261 (1993) 1280–1281.
[9] E.B. Babiychuk, A. Draeger, Annexins in cell membrane dynamics. Ca(2+)-regulated association of lipid microdomains, J. Cell Biol. 150 (2000) 1113–1124.
[10] N. Foger, R. Marhaba, M. Zoller, Involvement of CD44 in cytoskeleton rearrangement and raft reorganization in T cells, J. Cell Sci. 114 (2001) 1169–1178.
[11] Q. Tang, M. Edidin, Vesicle trafficking and cell surface membrane patchiness, Biophys. J. 81 (2001) 196–203.
[12] H. Heerklotz, Triton promotes domain formation in lipid raft mixtures, Biophys. J. 83 (2002) 2693–2701.
[13] N. Madore, K.L. Smith, C.H. Graham, A. Jen, K. Brady, S. Hall, R. Morris, Functionally different GPI proteins are organized in different domains on the neuronal surface, EMBO J. 18 (1999) 6917–6926.
[14] A.K. Kenworthy, M. Edidin, Distribution of a glycosylphosphatidylinositol-anchored protein at the apical surface of MDCK cells examined at a resolution of <100 A using imaging fluorescence resonance energy transfer, J. Cell Biol. 142 (1998) 69–84.
[15] A.K. Kenworthy, N. Petranova, M. Edidin, High-resolution FRET microscopy of cholera toxin B-subunit and GPI-anchored proteins in cell plasma membranes, Mol. Biol. Cell 11 (2000) 1645–1655.
[16] E.K. Fridriksson, P.A. Shipkova, E.D. Sheets, D. Holowka, B. Baird, F.W. McLafferty, Quantitative analysis of phospholipids in functionally important membrane domains from RBL-2H3 mast cells using tandem high-resolution mass spectrometry, Biochemistry 38 (1999) 8056–8063.
[17] F. Galbiati, B. Razani, M.P. Lisanti, Emerging themes in lipid rafts and caveolae, Cell 106 (2001) 403–411.
[18] S. Moffett, D.A. Brown, M.E. Linder, Lipid-dependent targeting of G proteins into rafts, J. Biol. Chem. 275 (2000) 2191–2198.
[19] A. Prinetti, V. Chigorno, G. Tettamanti, S. Sonnino, Sphingolipid-enriched membrane domains from rat cerebellar granule cells differentiated in culture. A compositional study, J. Biol. Chem. 275 (2000) 11658–11665.
[20] K.S. Koumanov, C. Tessier, A.B. Momchilova, D. Rainteau, C. Wolf, P.J. Quinn, Comparative lipid analysis and structure of detergent-resistant membrane raft fractions isolated from human and ruminant erythrocytes, Arch. Biochem. Biophys. 434 (2005) 150–158.
[21] K.A. Field, D. Holowka, B. Baird, Compartmentalized activation of the high affinity immunoglobulin E receptor within membrane domains, J. Biol. Chem. 272 (1997) 4276–4280.
[22] D.A. Brown, E. London, Functions of lipid rafts in biological membranes, Annu. Rev. Cell Dev. Biol. 14 (1998) 111–136.
[23] B. Baird, E.D. Sheets, D. Holowka, How does the plasma membrane participate in cellular signaling by receptors for immunoglobulin E? Biophys. Chem. 82 (1999) 109–119.
[24] M. Kawabuchi, Y. Satomi, T. Takao, Y. Shimonishi, S. Nada, K. Nagai, A. Tarakhovsky, M. Okada, Transmembrane phosphoprotein Cbp regulates the activities of Src-family tyrosine kinases, Nature 404 (2000) 999–1003.
[25] K.R. Solomon, E.A. Kurt-Jones, R.A. Saladino, A.M. Stack, I.F. Dunn, M. Ferretti, D. Golenbock, G.R. Fleisher, R.W. Finberg, Heterotrimeric G proteins physically associated with the lipopolysaccharide receptor CD14 modulate both in vivo and in vitro responses to lipopolysaccharide, J. Clin. Invest. 102 (1998) 2019–2027.
[26] F. Lafont, P. Verkade, T. Galli, C. Wimmer, D. Louvard, K. Simons, Raft association of SNAP receptors acting in apical trafficking in Madin-Darby canine kidney cells, Proc. Natl. Acad. Sci. U. S. A. 96 (1999) 3734–3738.
[27] W.B. Huttner, J. Zimmerberg, Implications of lipid microdomains for membrane curvature, budding and fission, Curr. Opin. Cell Biol. 13 (2001) 478–484.
[28] T.T. Markovska, T.N. Neicheva, A.B. Momchilova-Pankova, K.S. Koumanov, R. Infante, Effect of probucol on the lipid composition of blood plasma, erythrocyte ghosts and liver membranes in mice, Int. J. Biochem. 22 (1990) 1009–1013.
[29] E.G. Bligh, W.J. Dyer, A rapid method of total lipid extraction and purification, Can. J. Biochem. Physiol. 37 (1959) 911–917.
[30] W. Folkhard, D. Christmann, W. Geercken, E. Knorzer, M.H. Koch, E. Mosler, H. Nemetschek-Gansler, T. Nemetschek, Twisted fibrils are a structural principle in the assembly of interstitial collagens, chordae tendineae included, Z. Naturforsch., C 42 (1987) 1303–1306.
[31] C. Boulin, R. Kempf, A. Gabriel, M.H.J. Koch, S.M. McLaughlin, Data appraisal, evaluation and display for synchrotron radiation experiments: hardware and software, Nucl. Instrum. Methods A 249 (1986) 399–409.
[32] T.J. McIntosh, A. Vidal, S.A. Simon, Sorting of lipids and transmembrane peptides between detergent-soluble bilayers and detergent-resistant rafts, Biophys. J. 85 (2003) 1656–1666.
[33] B.Y. van Duyl, D.T. Rijkers, B. de Kruijff, J.A. Killian, Influence of hydrophobic mismatch and palmitoylation on the association of transmembrane alpha-helical peptides with detergent-resistant membranes, FEBS Lett. 523 (2002) 79–84.
[34] D. Furtado, W.P. Williams, A.P. Brain, P.J. Quinn, Phase separations in membranes of *Anacystis nidulans* grown at different temperatures, Biochim. Biophys. Acta 555 (1979) 352–357.
[35] R. Morris, H. Cox, E. Mombelli, P.J. Quinn, Rafts, little caves and large potholes: how lipid structure interacts with membrane proteins to create functionally diverse membrane environments, Subcell. Biochem. 37 (2004) 35–118.

[36] M.H. Wilkins, A.E. Blaurock, D.M. Engelman, Bilayer structure in membranes, Nat. New Biol. 230 (1971) 72–76.
[37] Y.K. Levine, M.H. Wilkins, Structure of oriented lipid bilayers, Nat. New Biol. 230 (1971) 69–72.
[38] B.A. Lewis, D.M. Engelman, Lipid bilayer thickness varies linearly with acyl chain length in fluid phosphatidylcholine vesicles, J. Mol. Biol. 166 (1983) 211–217.
[39] D.M. Engelman, Lipid bilayer structure in the membrane of *Mycoplasma laidlawii*, J. Mol. Biol. 58 (1971) 153–165.
[40] K. Mitra, I. Ubarretxena-Belandia, T. Taguchi, G. Warren, D.M. Engelman, Modulation of the bilayer thickness of exocytic pathway membranes by membrane proteins rather than cholesterol, Proc. Natl. Acad. Sci. U. S. A. 101 (2004) 4083–4088.
[41] Y. Feng, D. Rainteau, C. Chachaty, Z.W. Yu, C. Wolf, P.J. Quinn, Characterization of a quasicrystalline phase in codispersions of phosphatidylethanolamine and glucocerebroside, Biophys. J. 86 (2004) 2208–2217.
[42] D.G. Kakhniashvili, L.A. Bulla Jr., S.R. Goodman, The human erythrocyte proteome: analysis by ion trap mass spectrometry, Mol. Cell Proteomics 3 (2004) 501–509.
[43] S.R. Shaikh, V. Cherezov, M. Caffrey, W. Stillwell, S.R. Wassall, Interaction of cholesterol with a docosahexaenoic acid-containing phosphatidylethanolamine: trigger for microdomain/raft formation? Biochemistry 42 (2003) 12028–12037.
[44] D.A. Brown, E. London, Structure and origin of ordered lipid domains in biological membranes, J. Membr. Biol. 164 (1998) 103–114.
[45] A. Kusumi, I. Koyama-Honda, K. Suzuki, Molecular dynamics and interactions for creation of stimulation-induced stabilized rafts from small unstable steady-state rafts, Traffic 5 (2004) 213–230.
[46] E. London, Insights into lipid raft structure and formation from experiments in model membranes, Curr. Opin. Struct. Biol. 12 (2002) 480–486.
[47] S. Munro, An investigation of the role of transmembrane domains in Golgi protein retention, EMBO J. 14 (1995) 4695–4704.
[48] M. Gandhavadi, D. Allende, A. Vidal, S.A. Simon, T.J. McIntosh, Structure, composition, and peptide binding properties of detergent soluble bilayers and detergent resistant rafts, Biophys. J. 82 (2002) 1469–1482.
[49] H.A. Rinia, J.W. Boots, D.T. Rijkers, R.A. Kik, M.M. Snel, R.A. Demel, J.A. Killian, J.P. van der Eerden, B. de Kruijff, Domain formation in phosphatidylcholine bilayers containing transmembrane peptides: specific effects of flanking residues, Biochemistry 41 (2002) 2814–2824.